Modeling of high speed micro rotors in moderate flow confinement

E. Dikmen, P. J. M. van der Hoogt, R. G. K. M. Aarts
University of Twente, Institute of Mechanics, Processes and Control
Chair of Structural Dynamics and Acoustics
P.O. Box 217, 7500 AE, Enschede, Netherlands
email: **e.dikmen@utwente.nl**

Abstract

The recent developments in high speed micro rotating machinery lead to the need for multiphysical modeling of the rotor and the surrounding medium. In this study, thermal and flow induced effects on rotor dynamics of geometries with moderate flow confinement are studied. The structure is modeled via finite elements based on Timoshenko beams. Flow induced forces are implemented to the structure as added mass, stiffness and damping at each node. The temperature increase in the air gap, resulting from air friction is modeled via thermal networks in steady state as a function of rotation speed. The changed temperature affects the air properties and therefore the flow induced forces have to be recalculated. In this way, thermal and fluid effects in medium gap confinements are coupled with the rotordynamic model and their effects on critical speeds and vibration response can be investigated.

Nomenclature

c	damping of the fluid in the gap [Ns/m]
f	friction coefficient [-]
l	length of the shaft confined in fluid [m]
k	stiffness of the fluid in the gap [N/m]
m	mass of the fluid in the gap [kg]
m_a	added mass [kg]
r	radius of the shaft [m]
u_{x_i}	displacement of i^{th} node in x direction [m]
u_{y_i}	displacement of i^{th} node in y direction [m]
$\mathbf{q}$	vector of dof of the structure
$\mathbf{q_e}$	vector of dof of the element
$\mathbf{C}$	damping matrix [Ns/m]
$\mathbf{C_r}$	rotating damping matrix [Ns/m]
$\mathbf{f_n}$	non-rotating force vector [N]
$\mathbf{f_r}$	force vector caused by unbalance [N]
$\mathbf{G}$	gyroscopic matrix [kg] or [kgm^2]
$\mathbf{K}$	stiffness matrix [N/m]
L	length of fluid element [m]
$\mathbf{M}$	mass matrix [kg] or [kgm^2]
P	power loss due to air friction [W]
δ	clearance [m]
λ	complex frequency

μ viscosity [kg/m s]

ρ density of the fluid [kg/m^3]

ϕ_{x_i} angular displacement of ith node in x direction [rad]

ϕ_{y_i} angular displacement of ith node in y direction [rad]

ω rotation speed [rad/s]

1 Introduction

Due to developments in micro fabrication techniques, increasing demands for portable electronics and demands for faster micro production, the design and development of micro rotating machinery has been widely studied. A great number of researchers have been working on the development of devices such as micro electric motors, micro turbines and micro milling machines which include high speed rotating components. Therefore advanced rotordynamic models are required for the design of these components. However classical rotor dynamic modeling approaches can not be applied directly due to the multiphysical effects becoming crucial in micro level. Epstein et al. [1] state that viscous forces and fluid film heat transfer coefficients are higher in small scale and heat transfer becomes an important aspect of fluid mechanics, since micro devices operate in a different design space than large-scale machines. Similarly, Lin et al. [2] state that the air surrounding an oscillating microstructure has a profound effect on its dynamic behavior. Therefore multiphysical effects such as interaction with the surrounding air and thermal effects should be taken into account while examining the rotor dynamic behavior.

In this research work, temperature increase and fluid forces in the moderate confinements of high speed mini rotors are modeled. The reduced gap ratio (air gap/rotor radius) in these geometries is typically two orders of magnitude greater than the ones in small air gap geometries such as bearings and seals (0.1 to 0.001). Flow is generally turbulent as high speed rotors run in such confinements. Therefore inertial effects as well as viscous effects become significant. Antunes et al. [3] developed a theoretical model for flow induced forces in moderate flow confinement in terms of added mass, damping and stiffness. This model is used to simulate the rotordynamic behavior of a rigid rotor on flexible supports with two dof. In this study, constant air properties and friction coefficients in the confinement were used for the simulations.

In our study, the theoretical model for flow induced forces [3] is implemented to the rotor finite element model as a spring-damper and added mass at each node. Finite element modeling of the rotor is based on Timoshenko beams and each element has four degrees of freedom at each node. The temperature increase in the confinement is calculated and air properties and friction coefficients are updated. As the rotation speed increases, the heat loss due to friction and the temperature increase in the gap between rotor and stator become more significant. Consequently the change of air properties due to temperature increase in the gap should be considered when calculating the flow induced forces. The power generation in the gap due to friction is calculated by using empirical correlations and temperature increase is calculated by thermal networks which consist of resistances for rotor, stator and the gap. These results are used to calculate the air properties and friction coefficients which are required for calculating flow induced forces at each speed. In this way, the flow induced forces and the thermal effects are coupled with the structural model.

2 Modeling

2.1 Structural dynamics

Finite elements with a simple Timoshenko beam formulation [4], [5] taking shear deformation into account are used for modeling the rotor. Assuming uncoupled axial, torsional and flexural behavior, the number of dof becomes four at each node since only flexural behavior is taken into account.

Use of complex coordinates makes the calculations more convenient. The vector of nodal displacements of the element is: (2 translation and 2 rotational dof, see figure 1)

$$q_e = \left[u_{x_1} + iu_{y_1}, \phi_{y_1} - i\phi_{x_1}, u_{x_2} + iu_{y_2}, \phi_{y_2} - i\phi_{x_2}\right]^T \tag{1}$$

The schematic illustration of the element is given in figure 1. The consistent mass, stiffness and gyroscopic matrices of an element are described by Genta [4] in detail.

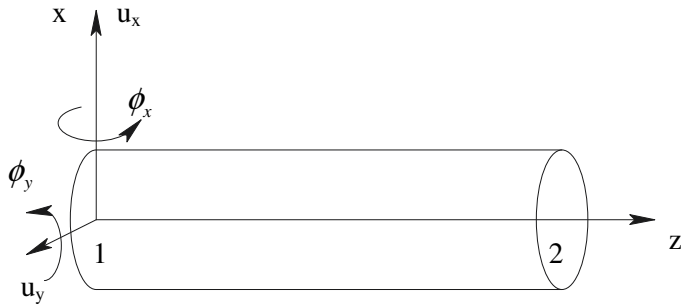

Figure 1: Degrees of freedom of a beam element

These matrices are assembled and the governing equations for the structure are obtained as [4]:

$$M\ddot{q} + (C - i\omega G)\dot{q} + (K - i\omega C_r)q = \omega^2 f_r e^{i\omega t} + f_n(t) \tag{2}$$

Where $f_r(t)$ and $f_n(t)$ are, the force caused by unbalance and a non-rotating force vector, respectively.

2.2 Flow induced forces

2.2.1 Formulation

The effect of the surrounding fluid on vibrations of the rotating shaft is widely studied. However most of the research work is done on small gap systems such as bearings and seals. The fluid flow in such geometries is generally laminar and Navier-Stokes equations are simplified to the Reynolds equation with some assumptions. However, less research results are available for larger gap geometries. For these configurations the gap to rotor radius ratios are around 0.1. [3]

In most of the micro rotating devices, there are moderate gaps between rotor and stator. Due to the high rotation speed, the flow inside these gaps is mostly turbulent.

The behavior of the flow in a gap between a rotating cylinder and casing depends on the Couette-Reynolds number and Taylor number defined as:

$$\mathrm{Re}_\delta = \frac{\rho\omega r\,\delta}{\mu} \qquad \text{and} \qquad Ta = \mathrm{Re}_\delta^2 \frac{\delta}{r} = \frac{\rho^2\omega^2 r\,\delta^3}{\mu^2} \tag{3}$$

If $\mathrm{Re}_\delta < 2000$ and Ta < 41, the basic two-dimensional Couette flow is observed; when $\mathrm{Re}_\delta < 2000$ and Ta > 41, the flow is still laminar but displays three-dimensional Taylor vortices; when $\mathrm{Re}_\delta > 2000$, the flow becomes turbulent. For this case a detailed model of the flow is quite complex. Therefore the following assumptions are commonly made for simplifying the governing equations: (a) the flow is assumed to be incompressible and two dimensional; (b) the turbulent shear stresses are modeled using semi empirical friction coefficients [3]. The flow field is given in figure 2.

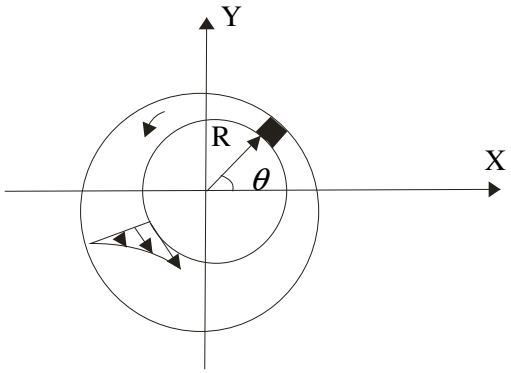

Figure 2: Two dimensional annular flow

Antunes et. al. [3] obtained linearized fluid forces per unit length for both concentric and eccentric fluid annulus with medium gap by using perturbation methods with the above assumptions. The obtained forces were added to a simple rotordynamic model with a rigid rotor and flexible supports. Then, simulations with different eccentricities were performed and verified experimentally. In the present study, this model is implemented to the structural finite element model and coupled with a thermal model enabling updated friction and air properties at different rotation speeds.

2.2.2 Coupling with FEM

The fluid forces per unit length for concentric configuration are:

$$\begin{Bmatrix} f_x \\ f_y \end{Bmatrix} = \begin{bmatrix} m_a & 0 \\ 0 & m_a \end{bmatrix} \begin{Bmatrix} \ddot{u}_x \\ \ddot{u}_y \end{Bmatrix} + \begin{bmatrix} c_{xx} & c_{xy} \\ -c_{xy} & c_{xx} \end{bmatrix} \begin{Bmatrix} \dot{u}_x \\ \dot{u}_y \end{Bmatrix} + \begin{bmatrix} k_{xx} & k_{xy} \\ -k_{xy} & k_{xx} \end{bmatrix} \begin{Bmatrix} u_x \\ u_y \end{Bmatrix} \tag{4}$$

Where $m_a = \frac{\pi r^3 \rho}{\delta}, c_{xx} = \frac{\omega}{\delta} f\, m_a, c_{xy} = \omega m_a, k_{xx} = -\frac{\omega^2 m_a}{4},\ k_{xy} = -\frac{\omega^2 m_a}{4}$ (5)

With some algebra these equations can be written in complex coordinates:

$$m_a \ddot{u}_x + c_{xx}\dot{u}_x + c_{xy}\dot{u}_y + k_{xx}u_x + k_{xy}u_y = 0$$

$$i(m_a \ddot{u}_y + c_{xx}\dot{u}_y - c_{xy}\dot{u}_x - k_{xy}u_x + k_{xx}u_y = 0)$$

$$m_a(\ddot{u}_x + i\ddot{u}_y) + c_{xx}(\dot{u}_x + i\dot{u}_y) - ic_{xy}(\dot{u}_x + i\dot{u}_y) + k_{xx}(u_x + iu_y) - ik_{xy}(u_x + iu_y) = 0 \tag{6}$$

The governing equations for the structure in the absence of unbalance and non-rotating force are given in section 2.1. as:

$$M\ddot{q} + (C - i\omega G)\dot{q} + (K - i\omega C_r)q = 0 \tag{7}$$

The fluid forces in equation (6) are multiplied with element length L and lumped to the nodes of each element. The added mass m_a is assembled to the mass matrix M, the damping c_{xx} to the damping matrix C and the stiffness k_{xx} to the stiffness matrix K, the damping c_{xy} is assembled to the gyroscopic matrix G and the stiffness k_{xy} to rotating damping matrix C_r.

2.3 Thermal model

The turbulent flow not only affects rotor dynamics of the shaft but also causes large amounts of power loss due to high rotation speeds. The friction loss in the gap is determined by the velocity field and the air properties. The fluid velocity field is calculated by the Navier-Stokes and the continuity equations. These equations can be solved analytically for simple geometries in laminar flow. However for turbulent flow, these equations become more difficult to solve. Therefore, semi empirical friction coefficients are commonly used to describe the friction loss for turbulent flows. In this study, air friction loss is calculated by semi empirical correlations which are functions of the Reynolds number and thermal resistance networks are used to calculate the temperature in the air gap.
Correlations provided by Bilgen and Boulos [6] are used to calculate friction coefficients:

$$f = 0.515 \frac{\left(\frac{\delta}{r}\right)^{0.3}}{\mathrm{Re}_{\delta}^{0.5}} \qquad (500<\mathrm{Re}_{\delta}<10^4) \tag{8}$$

$$f = 0.0325 \frac{\left(\frac{\delta}{r}\right)^{0.3}}{\mathrm{Re}_{\delta}^{0.2}} \qquad (10^4<\mathrm{Re}_{\delta}) \tag{9}$$

These empirical friction coefficients are used to calculate the power loss, given by:

$$P_f = f\pi\rho\omega^3 r^4 l \tag{10}$$

The temperature in the gap is determined by thermal networks which involve nodes describing the mean temperature of each component and resistances among them. All the heat generation in the component is applied to the node describing the component. Figure 3 illustrates independent axial and radial networks.
In this study a thermal network corresponding to a simple rotor stator system is constructed by using the component resistances developed by Saari [7], [8].
A simple Matlab based code is developed for the calculation of air friction and temperature increase. The material properties, dimensions and rotation speed are inputs of the program. The convection heat transfer coefficients are calculated in the program and used for determination of the resistances. The temperature of the air in the gap and total power loss are the outputs of the program.

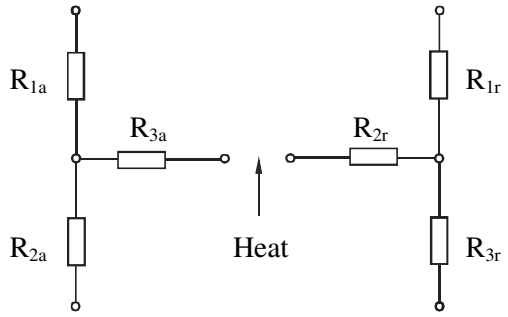

Figure 3: Independent axial and radial thermal resistances

At a specific rotation speed heat generation and fluid temperature is obtained. This temperature is used to update friction coefficients and fluid properties which are required for calculation of the flow induced forces. In this way; a coupled analysis of three physical domains is performed.

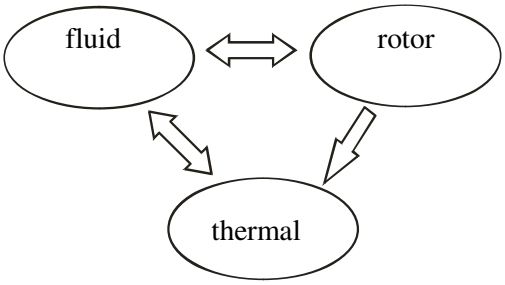

Figure 4: Interaction between physical domains

3 Simulation Results

The thermal and fluid effects are investigated for different geometries, various gap sizes and different bearing stiffness. The dimensions of the rotor used in the simulations are given in Figure 5. The disc with a diameter of 40 mm is confined with a casing.

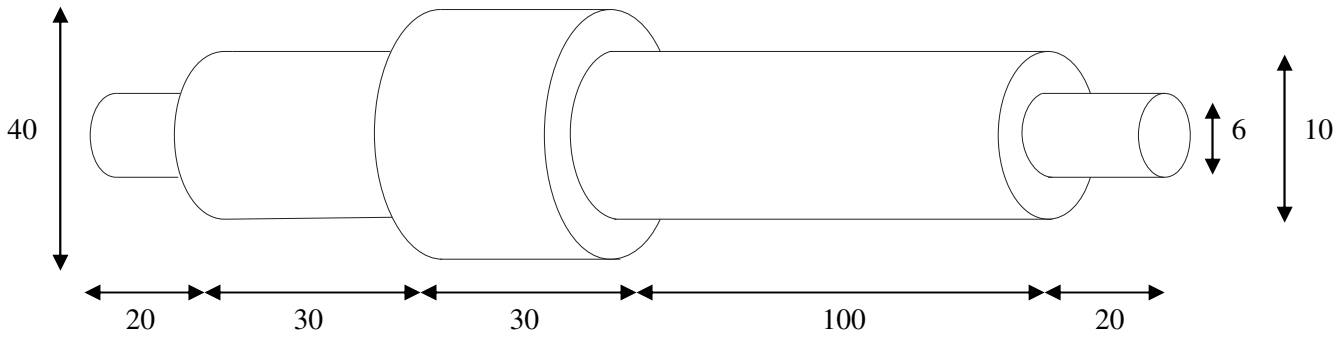

Figure 5: Dimensions (mm) of the rotor used in the simulations

In table (1), the natural frequencies related with the first rigid body mode and flexible mode of the above rotor are provided with different gap dimensions. (supports on each side with a stiffness of 10^5 N/m)

Natural frequencies of the first rigid body and first flexible mode (rad/s) for different clearances (Bearing stiffness = 10^5 N/m) at 100 000 rpm				
	Without fluid	δ=0.25 mm	δ =0.5 mm	δ =1 mm
Rigid Body	677	532	597	638
Flexible	10 562	10 560	10 560	10 560

Table 1: Natural frequencies for different gap dimension

As the gap decreases the flow induced effects become much more important. Flow induced effects are also investigated for different support stiffness. As the stiffness decreases, the effects are much more pronounced. The change of the natural frequencies with different support stiffness is illustrated in Table 2.

Natural frequencies of the first rigid body and first flexible mode (rad/s) for different stiffness (δ =0.5 mm) at 100 000 rpm						
	k= 10^4 N/m		k= 10^5 N/m		k= 10^6 N/m	
	Without Fluid		Without Fluid		Without Fluid	
Rigid Body	220	111	677	597	1 659	1 656
Flexible	10 340	10 339	10 562	10 560	12 522	12 520

Table 2: Natural frequencies for different support stiffness

The stiffness of the bearings is significant for the change of the first rigid body mode. As the stiffness decreases, the flow induced effects become more important.

Figure (6) illustrates the change of the first natural frequency as a function of rotation speed at different stiffness.

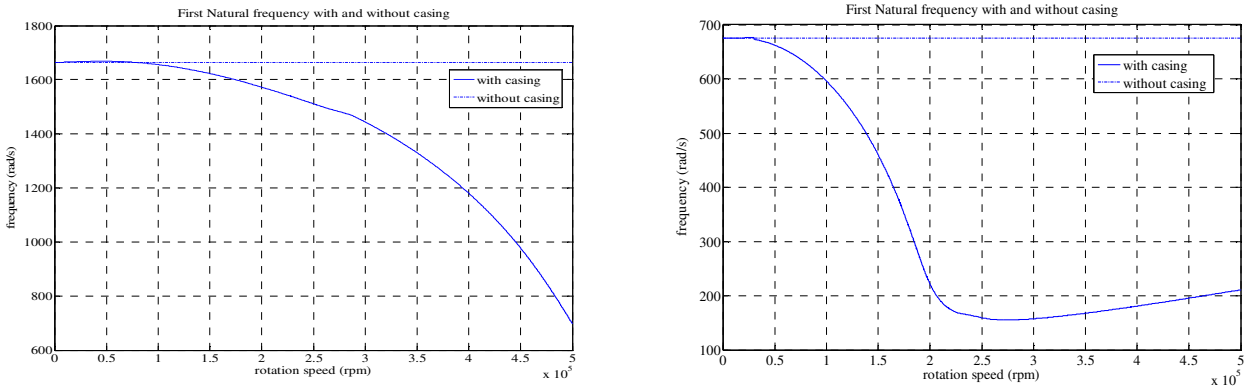

Figure 6: Change of first natural frequency at different rotation speeds with bearing stiffness of a) 10^6 N/m and b) 10^5 N/m

Finally, the effect of the surface velocity is investigated by decreasing the disc diameter from 40 mm to 10 mm (with δ=0.5 mm). As shown in table 3, the natural frequency of the first rigid body mode is considerable, even with low stiffness of the supports.

Natural frequencies of the first rigid body and first flexible mode (rad/s) for different disc diameters with k= 10^5 N/m				
	dia=10 mm		dia= 40 mm	
	Without Fluid		Without Fluid	
Rigid Body	1315	1316	673	597
Flexible	9342	9340	10 562	10 560

Table 3: Change of first natural frequency with different disc diameter

The fluid forces have also components that contribute to the rotational damping matrix C_r, resulting in self-excited vibrations. The non-rotating damping in the supports is important for stable operation. Decay rates (imaginary part of the complex frequency λ where $e^{i\lambda t}$ is the solution of equation of motion) for different support damping are given below. With a viscous damping coefficient of 1 Ns/m, stable

operation is achieved up to 50 000 rpm for the geometry given in figure 5. As the damping of the supports increase, the stable operation range increases as can be expected. (for 10 Ns/m up to 140 000 rpm)

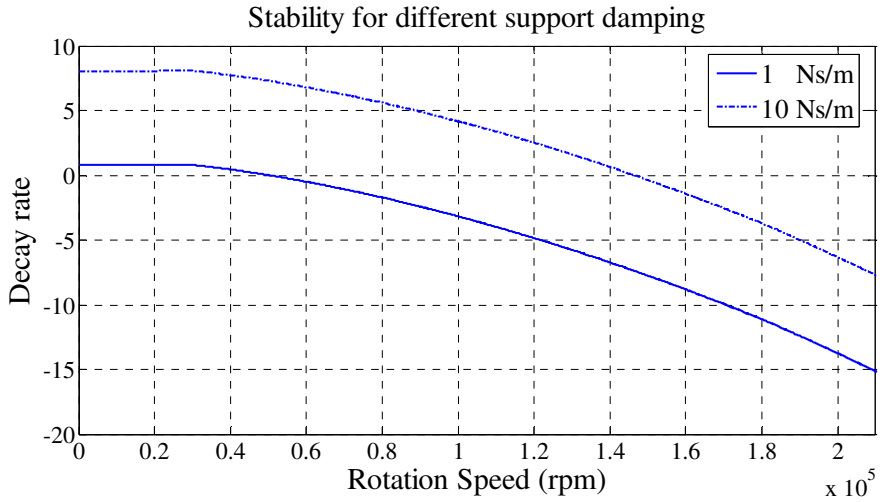

Figure 7: Stability analysis for different support damping

4 Conclusion and Future Work

The fluid effects on rotordynamics of high speed shafts with moderate air gap are outlined. Structural, fluid and thermal models are coupled to each other. The surrounding air has almost no effect on the *flexural* natural frequency however it affects the *rigid* body frequency. The influence becomes more pronounced when the stiffness of the supports and the gap decrease. The presence of the surrounding air may also result in stability problems depending on the ratio of the rotating and non-rotating damping. Future work involves construction of a high speed rotating experimental setup in order to verify the developed models.

References

[1] A. Epstein, *Millimeter-Scale, Micro Electro-Mechanical Systems Gas Turbine Engines,* Journal of Engineering for Gas Turbines and Power, Vol. 126, (2004), pp. 205-226.

[2] R.M. Lin, W.J. Wang, *Structural dynamics of microsystems—current state of research and future directions,* Mechanical Systems and Signal Processing, Vol. 20, (2006), pp. 1015–1043.

[3] J. Antunes, F. Axisa, T. Grunenwald, *Dynamics of rotors immersed in eccentric annular flow: Part [1]: Theory*, Journal of Fluids and Structures, Vol. 10, (1996), pp. 897-918.

[4] G. Genta, *Dynamics of Rotating Systems,* Springer, New York, (2005).

[5] G.Genta, *Consistent matrices in rotor dynamics,* Meccanica, Vol. 20, (1985), pp.235-248.

[6] E. Bilgen, R.Boulos, *Functional dependence of torque coefficient of coaxial cylinders on gap width and Reynolds numbers,* Transactions of ASME, Journal of Fluids Engineering, Vol. 95, No.1, (1973), pp.122-126.

[7] J. Saari, *Thermal analysis of high-speed induction machines,* Acta Polytechnica Scandinavica, Electrical Engineering Series No. 90, Helsinki, (1998).

[8] J. Saari, *Thermal modeling of high-speed induction machines*, Acta Polytechnica Scandinavica, Electrical Engineering Series No.82. Helsinki, (1995).